

ConcealGS: Concealing Invisible Copyright Information in 3D Gaussian Splatting

Yifeng Yang^{1†}, Hengyu Liu^{2†}, Chenxin Li^{2‡}, Yining Sun³, Wuyang Li²
Yifan Liu², Yiyang Lin², Yixuan Yuan^{2*}, Nanyang Ye^{1*}

¹Shanghai Jiao Tong University ²The Chinese University of Hong Kong ³Johns Hopkins University

Abstract—As 3D Gaussian Splatting (3D-GS) emerges as a promising technique for 3D reconstruction and novel view synthesis, offering superior rendering quality and efficiency, it becomes crucial to ensure secure transmission and copyright protection of 3D assets in anticipation of widespread distribution. While steganography has advanced significantly in common 3D media like meshes and Neural Radiance Fields (NeRF), research into steganography for 3D-GS representations remains largely unexplored. To address this gap, we propose ConcealGS, a novel 3D steganography method that embeds implicit information into the explicit 3D representation of Gaussian Splatting. By introducing a consistency strategy for the decoder and a gradient optimization approach, ConcealGS overcomes limitations of NeRF-based models, enhancing both the robustness of implicit information and the quality of 3D reconstruction. Extensive evaluations across various potential application scenarios demonstrate that ConcealGS successfully recovers implicit information with negligible impact on rendering quality, offering a groundbreaking approach for embedding invisible yet recoverable information into 3D models. This work paves the way for advanced copyright protection and secure data transmission in the evolving landscape of 3D content creation and distribution. Code is available at <https://github.com/zxk1212/ConcealGS>.

Index Terms—Gaussian Splatting, Steganography, 3D reconstruction

I. INTRODUCTION

Steganography, a technique for concealing information within digital media formats [1]–[3] such as images, audio files, videos, and text documents, has been widely used for copyright protection, content authentication, and secure information transfer. While traditionally focused on embedding data in images or videos, the growing ubiquity of digital content has spurred demand for more sophisticated steganographic methods. As 3D representations continue to advance, we anticipate a future where sharing 3D content captured from real-world environments or modeled in virtual spaces becomes as commonplace as sharing 2D media online, opening new avenues for steganographic applications.

Advanced methods for hiding information in 3D representations primarily utilize Implicit Neural Representation (INR) [4]–[7], which conceptualizes images and neural networks as functions [8]–[10]. INR expresses high-dimensional information with few parameters, enabling efficient information embedding [11] and enhancing robustness against processing operations [4], [12], [13]. Building on this, [14] introduced Neural Radiance Field (NeRF) for realistic 3D scene renderings. StegaNeRF [6] further leverages multilayer perceptrons to simulate light propagation,

reconstruct 3D scenes from multiview images, and embed implicit information in MLP weights, using U-Net [15], [16] for decoding. However, these methods are limited by their reliance on NeRF, tying the quality of rendered images and hidden information to NeRF’s capabilities.

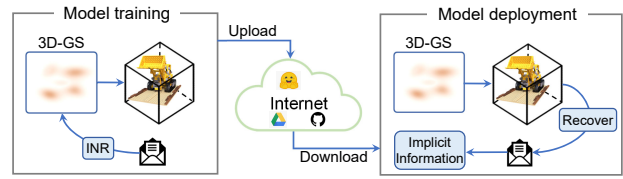


Fig. 1. Illustration of the proposed copyright protection process using 3D-GS. Left: During model training, the owner embeds implicit information into the 3D-GS parameters and uploads the model. Right: During model deployment, when the shared model is used (potentially for commercial purposes), the owner can recover the embedded information from rendered images to identify copyright infringement.

Recently, advanced methods based on 3D Gaussian Splatting (3D-GS) [17] have gained popularity. Unlike NeRF, 3D-GS represents point clouds in 3D space using Gaussian distributions, achieving 3D reconstruction with fewer parameters. Recent studies [18]–[23] have demonstrated that 3D-GS generally leads to more efficient and higher-quality 3D representations across various tasks compared to NeRF. Given this promise, we are eager to open the exploration for the following research questions:

- ▷ **Workable Embedding:** Can we effectively embed implicit information into 3D-GS learnable parameters?
- ▷ **Comparative Analysis:** How does implicit information embedding in 3D-GS compare to NeRF’s MLP-based implicit neural representation in terms of performance and impact on the 3D model?
- ▷ **Robustness to Retraining:** Can the embedded information be retained after re-training on additional data?

To address the aforementioned questions, we consider the following scenario: As illustrated in Figure 1, during the training phase, the owner embeds implicit information into the learnable parameters of the 3D-GS and completes the 3D reconstruction. Subsequently, the reconstructed 3D representation is shared on the internet. Other users can then download and deploy this 3D representation. When the owner observes their shared 3D representation being used for commercial purposes, they can utilize a custom module to recover the embedded implicit information from the rendered images. The successful recovery of this embedded information can serve as evidence to determine whether an infringement has occurred.

Built on the superior rendering quality and rendering speed of 3D-GS [17], we propose **ConcealGS**: a 3D

[†]Equal contribution, [‡]Project Lead, ^{*}Corresponding author.

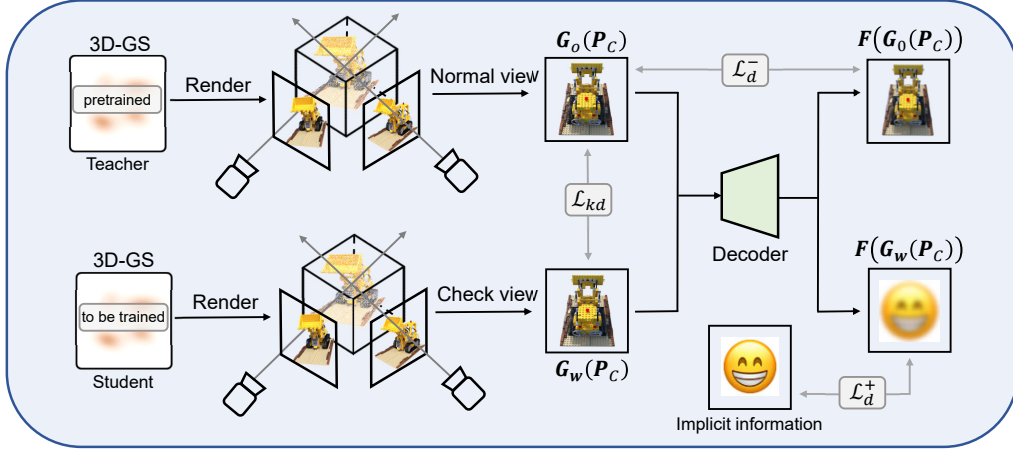


Fig. 2. Overview of ConcealGS: The process involves two key stages. (1) Pre-training: A 3D-GS model is pre-trained as a teacher model for high-quality image rendering. (2) Training: Guided by the teacher model, we simultaneously train a student model and a decoder. The student model learns to render images with embedded implicit information, while maintaining visual similarity to the teacher’s output. A gradient-guided optimization strategy, detailed in Section II-C, is employed to balance rendering quality and information embedding effectiveness.

steganography method which embeds implicit information into the 3D explicit representation of Gaussian Splatting with almost no rendering quality decline. We use a decoder to detect the implicit information. To maintain the render quality, we distill knowledge [24], [25] from a pretrained model to ConcealGS. A consistency strategy is proposed for implicit information embedding. During optimization, we use a Gradient Guided Optimization strategy to balance the quality of the rendering and hidden recovery. Extensive experimental results demonstrate that the proposed method significantly outperforms NeRF-based steganography methods in both 3D reconstruction quality and the efficiency of implicit information recovery. This advancement not only enhances the potential for digital rights management in 3D content but also opens new avenues for secure information transmission within complex 3D representations.

II. METHOD

In this section, we elaborate the proposed implicit information embedding method: ConcealGS. We first outline the fundamental principles of 3D Gaussian splatting in Sec. II-A. In Sec. II-B, we propose a knowledge distillation framework to embed implicit information, with a rendering consistency loss and a contrastive loss to learn effectively. In Sec. II-C, we propose a gradient-guided optimization strategy which dynamically adjusts the gradient weights of the decoder layers to balance the two objectives. The overview of the ConcealGS can be referred to in Fig. 2.

A. Preliminaries: Representation of 3D Gaussian

3D-GS [17] employs a collection of Gaussians with various attributes to represent 3D data. Specifically, each Gaussian is defined by a covariance matrix Σ and a center point $\mathbf{X} \in \mathbb{R}^3$, where is the mean value of the Gaussian:

$$G(\mathbf{X}) = e^{-\frac{1}{2}\mathbf{X}^T\Sigma^{-1}\mathbf{X}}, \quad (1)$$

where Σ can be decomposed into a scaling factor $\mathbf{s} \in \mathbb{R}^3$ and a rotation quaternion $\mathbf{q} \in \mathbb{R}^4$ for differentiable optimization. The rendering of 3D Gaussians entails their

projection onto the image plane as 2D Gaussians [26]. The blending of ordered points for the overlap pixel can be calculated by:

$$C = \sum_{i \in N} c_i \alpha_i \prod_{j=1}^{i-1} (1 - \alpha_j), \quad (2)$$

where $\alpha \in \mathbb{R}$, $\mathbf{c} \in \mathbb{R}^C$ represent the opacity value and color feature, with spherical harmonics employed to capture view-dependent effects. These parameters are collectively denoted as \mathbf{G} , where $\mathbf{G}_i = \{\mathbf{X}_i, \mathbf{s}_i, \mathbf{q}_i, \alpha_i, \mathbf{c}_i\}$ denotes the parameters for the i -th Gaussian.

B. Implicit Information embedding and covering

Rendering Consistency. Directly training a 3D representation that incorporates implicit information can substantially degrade the quality of the rendered images [6]. To address this, we utilize a knowledge distillation [24], [25] strategy to maintain the rendering quality while incorporating implicit information and transferring knowledge from a pretrained model. In this process, a pre-trained 3D Gaussian (teacher model) guides the student model with implicit information to ensure the rendered images on known poses are not overly altered. The knowledge distillation regularization term \mathcal{L}_{kd} is defined as:

$$\mathcal{L}_{kd} = |\mathbf{G}_w(\mathbf{P}_m) - \mathbf{G}_o(\mathbf{P}_m)| \quad (3)$$

where $\mathbf{G}_w(\mathbf{P}_m)$ and $\mathbf{G}_o(\mathbf{P}_m)$ represent check rendered image at the camera position \mathbf{P}_m of the student model and teacher model.

Decoding Consistency. ConcealGS uses a universal decoder F to decode implicit information from check view \mathbf{P}_c rendering and original image from normal view $\mathbf{P}_n \in \{\mathbf{P}_{nj}\}_{j=1}^M$ [27]. To minimize the rendering quality decline on normal view, the decoder is trained as an identity network on normal view \mathbf{P}_n :

$$\mathcal{L}_d^- = |F(\mathbf{G}_o(\mathbf{P}_n)) - \mathbf{G}_o(\mathbf{P}_n)| \quad (4)$$

\mathcal{L}_d^- ensures that the difference between the output of the decoder and normal view remains very small. This makes the decoder’s input and output as consistent as possible

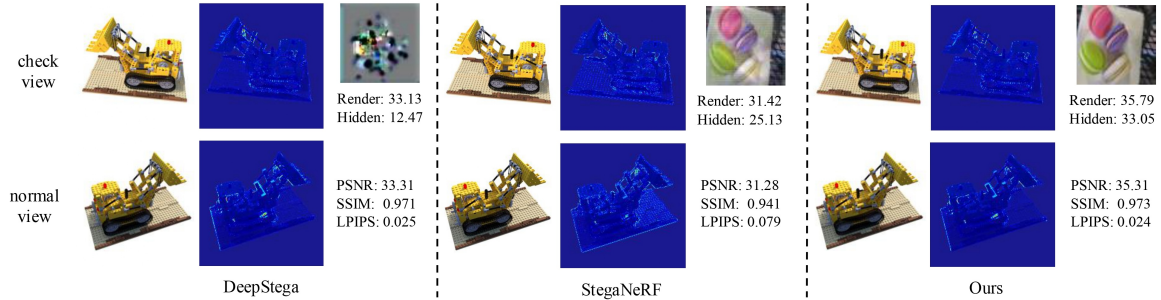


Fig. 3. Qualitative comparison on NeRF-Synthetic [14]. Within each column, we show the rendering images on check view and normal view, the recovered hidden image and the residual error compared to the ground truth image. We present the PSNR for scene renderings and recovered hidden images from the check view, along with the PSNR, SSIM, and LPIPS metrics for scene renderings from the normal view.

when normal view are used as input, thereby introducing only minimal changes or noise.

Implicit Information processing. ConcealGS encodes implicit information into the 3D explicit representation by supervising the output of the decoder on check view P_c . Specifically, we minimize the loss between the output of the decoder on check view P_c and the ground truth of the implicit information:

$$\mathcal{L}_d^+ = |\mathbf{F}(\mathbf{G}_w(P_c)) - \mathbf{I}| \quad (5)$$

where \mathbf{I} is the target embedded implicit information and \mathcal{L}_d^+ measures the difference between the predicted implicit information and \mathbf{I} . Through optimization, implicit information can be recovered from rendered image on check view, which indicates the implicit information is embedded in the 3D explicit representation.

C. Gradient Guided Optimization

During optimization, the process of embedding implicit information and strategy of decoding consistency will make the universal decoder trapped in the trade-off of decoding implicit information on check view (\mathcal{L}_d^+ in Eq 5) and maintaining the consistency of the normal view (\mathcal{L}_d^- in Eq 4). To ensure that decoder effectively extracts implicit information while preserving the integrity of the rendering image and minimizing gradient conflicts, a gradient-guided optimization strategy is utilized by ConcealGS. This strategy dynamically enhances or suppresses parameter updates in specific layers by measuring the similarity between the gradients of positive and negative contrastive loss functions.

For decoder \mathbf{F} with N layers: $\{f_i\}_{i=1}^N$, the gradients of each layer f_i with respect to \mathcal{L}_d^+ , \mathcal{L}_d^- are denoted by $\nabla_{f_i} \mathcal{L}_d^+$ and $\nabla_{f_i} \mathcal{L}_d^-$, respectively. We use the cosine similarity between $\nabla_{f_i} \mathcal{L}_d^+$ and $\nabla_{f_i} \mathcal{L}_d^-$, to calculate the emphasis of the current parameters on the two mentioned tasks:

$$s_i = \frac{\langle \nabla_{f_i} \mathcal{L}_d^+, \nabla_{f_i} \mathcal{L}_d^- \rangle}{\|\nabla_{f_i} \mathcal{L}_d^+\| \|\nabla_{f_i} \mathcal{L}_d^-\|}, w_i = \sigma(s_i) \quad (6)$$

s_i is passed through the sigmoid function σ to obtain the weight for each layer's gradient. During optimization, the gradient of each layer $\frac{\partial \mathcal{L}}{\partial f_i}$ is multiplied by the corresponding gradient weight w_i before updating:

$$\frac{\partial \mathcal{L}}{\partial f_i} \leftarrow w_i \cdot \frac{\partial \mathcal{L}}{\partial f_i}, \quad \forall i \in \{1, 2, \dots, N\} \quad (7)$$

Specifically, the layer with similar gradients indicates that it processes both tasks in a relatively consistent direction, meaning no significant adjustment is needed. If the gradients are dissimilar, it suggests a large discrepancy in how the layer handles the tasks, requiring suppression of the update. This dynamic adjustment mechanism coordinates the conflicting losses across different layers of the decoder, thus achieving the dual goals of implicit information extraction and the original rendering image preservation.

TABLE I
QUANTITATIVE RESULTS OF RENDERING PERFORMANCE AND HIDDEN INFORMATION RECOVERY ON NeRF-SYNTHETIC [14].

Methods	Scene Rendering			Hidden Recovery	
	PSNR \uparrow	SSIM \uparrow	LPIPS \downarrow	PSNR \uparrow	SSIM \uparrow
3D-GS [17]	34.45	0.9732	0.0220	-	-
LSB [28]	33.05	0.9704	0.0253	6.13	0.1218
DeepStega [29]	33.06	0.9702	0.0253	11.13	0.2265
StegaNeRF [6]	30.33	0.9381	0.0787	24.60	0.9026
ours	33.14	0.9717	0.0240	33.98	0.9942

TABLE II
QUANTITATIVE RESULTS OF RENDERING PERFORMANCE AND HIDDEN INFORMATION RECOVERY ON T&T [17].

Methods	Scene Rendering			Hidden Recovery	
	PSNR \uparrow	SSIM \uparrow	LPIPS \downarrow	PSNR \uparrow	SSIM \uparrow
3D-GS [17]	27.43	0.9190	0.0779	-	-
LSB [28]	26.11	0.8994	0.1048	5.98	0.0826
DeepStega [29]	26.17	0.9000	0.1047	6.27	0.1532
StegaNeRF [6]	23.48	0.7462	0.6067	32.33	0.9918
ours	27.26	0.9177	0.0796	37.53	0.9935

III. EXPERIMENTS

A. Experimental Settings

Datasets and Metrics. We utilize two widely recognized datasets: NeRF-Synthetic [14] and T&T as used in [17]. We select four 360° scenes $\{lego, drums, chair, ship\}$ from NeRF-Synthetic. The T&T dataset includes four scenes: $\{playroom, drjohnson, truck, train\}$. We adopt the same data splitting as described in [17]. Following [6], [30], we evaluate the quality of the hidden information recovered by the decoder using two metrics: PSNR and SSIM. We employ PSNR, SSIM, and LPIPS as metrics for rendering quality of 3D-GS.

Implementation Details. We set the resolution of the hidden image to $[64, 64]$ and with the same data as [6], [30]. Following [6], [30], a simple U-Net [15] is utilized as the decoder for hidden information and the learning rate of the detector is set to $1e^{-4}$. Other settings and parameters on NeRF-Synthetic and T&T are the same as [17].

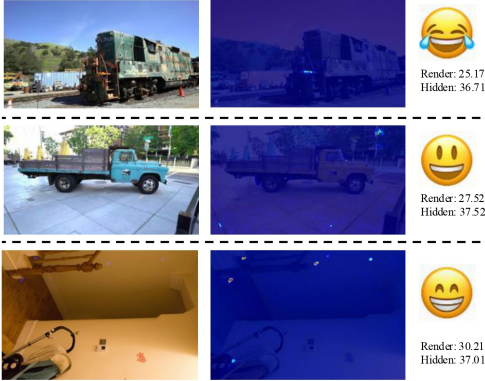


Fig. 4. Results on the T&T [17]. Each row displays scene rendering, residual error compared to ground truth image, and the recovered hidden image. We present the PSNR of scene rendering and hidden recovery.

B. Experimental Results

We use three widely recognized techniques: LSB [28], DeepStega [29], and StegaNeRF [6] for comparison. Experimental results on NeRF-Synthetic [14] and T&T [17] are respectively shown in Tab. I and Tab. II. We observe that traditional methods, such as LSB [28] and DeepStega [29], achieve reasonable scene rendering quality with PSNR values exceeding 26. However, they struggle with hidden information recovery, exhibiting significantly lower PSNR across both datasets. In contrast, StegaNeRF [6] effectively hides information in 3D representations. However, it compromises scene rendering quality, resulting in a PSNR that is 3 lower than ours. ConcealGS demonstrates a PSNR improvement of 0.89 and 5.20 over other methods in scene rendering and hidden recovery.

Compared to standard 3D-GS model (without adding any hidden information), our methods only have a 0.17 lower PSNR and 0.0013 lower SSIM, which indicates that ConcealGS successfully conceals implicit information in the 3D representation with almost no performance decline. Visual results are shown in Fig. 3 and Fig. 4, which also demonstrates that our approach not only provides superior rendering quality but also significantly enhances hidden information recovery compared to other methods.

C. Ablation Studies

To prove the effectiveness of each component of our method, we conduct ablation experiments on the T&T [17] dataset and experimental results are presented in Tab. III, where *w.o. decoder* means directly recover hidden message from check pose without the decoder, *w.o. consis.* devotes our methods without the consistency strategy proposed in Sec. II-B, and *w.o. grad.* devotes the model without the gradient guided optimization proposed in Sec. II-C. We can observe that the use of decoder can help prevent the model from overfitting on the hidden information to protect scene rendering performance. The use of the

consistency strategy and the gradient guided optimization enables our method adaptively updated according to the influence of different losses during the optimization process to achieve a good trade-off between the performance of the rendering scene and the hidden recovery.

TABLE III
ABLATION STUDY OF DIFFERENT COMPONENTS OF CONCEALGS.
RESULTS ARE CONDUCTED ON T&T [17].

Methods	Scene Rendering			Hidden Recovery	
	PSNR \uparrow	SSIM \uparrow	LPIPS \downarrow	PSNR \uparrow	SSIM \uparrow
Ours	27.26	0.9177	0.0796	37.53	0.9935
w.o. Decoder	26.25	0.8965	0.0884	37.56	0.9948
w.o. Consis.	25.74	0.8542	0.1265	37.13	0.9924
w.o. Grad.	26.93	0.9043	0.0812	37.43	0.9912
3D-GS	27.43	0.9190	0.0779	-	-

D. Robustness Analysis

The results of robustness analysis are shown in Fig. 5, where the image is scaled in $[0, 1]$ and a higher JPEG ratio means more information from the original image is retained. The SSIM values reflect mean performance across varying conditions (only 0.02 decreased). These results suggest that the method effectively maintains the integrity of hidden information, when subjected to Gaussian Blur and JPEG compression, which indicates that our method could remain robust under the application in real-world and complex environments with various noises.

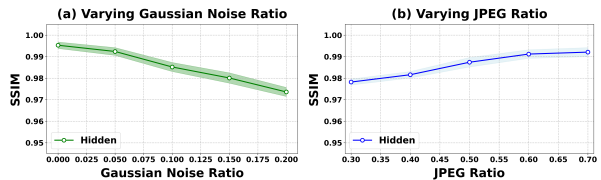


Fig. 5. Robustness Analysis over various (a) Gaussian blur and (b) JPEG compression ratio. SSIM of hidden recovery on T&T [17] is shown.

IV. CONCLUSION

As 3D content increasingly becomes a core component of various applications, it is crucial to explore methods for embedding information into 3D-GS. In this paper, we propose ConcealGS, which embeds implicit information into the 3D explicit representation with almost no rendering quality decline. Experimental results have shown that our method outperforms other steganography methods in both rendering quality and efficiency, as well as implicit information recovery. Extension studies demonstrate that the key components required to implement the technique are effective, and investigate the effectiveness of embedding implicit information into 3D-GS and its impact on rendering quality. This paper introduces a novel exploration of ownership identification within the framework of Gaussian Splatting, highlighting the need for increased attention and effort dedicated to related issues.

REFERENCES

- [1] Jas Kaur and Jagroop Kaur, "Hiding text in video using steganographic technique-a review," *International Journal of Engineering Sciences*, vol. 17, no. 1, pp. 578–582, 2016.
- [2] Jayakanth Kuntho, Nandhini Subramanian, Somaya Al-Maadeed, and Ahmed Bouridane, "Video steganography: recent advances and challenges," *Multimedia Tools and Applications*, vol. 82, no. 27, pp. 41943–41985, 2023.
- [3] B Delina, "Information hiding: A new approach in text steganography," in *Proceedings of the International Conference on Applied Computer and Applied Computational Science, World Scientific and Engineering Academy and Society (WSEAS 2008)*, 2008, pp. 689–695.
- [4] Youngdong Jang, Dong In Lee, MinHyuk Jang, Jong Wook Kim, Feng Yang, and Sangpil Kim, "Waterf: Robust watermarks in radiance fields for protection of copyrights," in *Proceedings of the IEEE/CVF Conference on Computer Vision and Pattern Recognition*, 2024, pp. 12087–12097.
- [5] Jia Liu, Peng Luo, and Yan Ke, "Hiding functions within functions: Steganography by implicit neural representations," *arXiv preprint arXiv:2312.04743*, 2023.
- [6] Chenxin Li, Brandon Y Feng, Zhiwen Fan, Panwang Pan, and Zhangyang Wang, "Steganerf: Embedding invisible information within neural radiance fields," in *Proceedings of the IEEE/CVF International Conference on Computer Vision*, 2023, pp. 441–453.
- [7] Win Kent Ong, Kam Woh Ng, Chee Seng Chan, Yi Zhe Song, and Tao Xiang, "Ipr-nerf: Ownership verification meets neural radiance field," *arXiv preprint arXiv:2401.09495*, 2024.
- [8] Jeong Joon Park, Peter Florence, Julian Straub, Richard Newcombe, and Steven Lovegrove, "Deepssf: Learning continuous signed distance functions for shape representation," in *Proceedings of the IEEE/CVF conference on computer vision and pattern recognition*, 2019, pp. 165–174.
- [9] Zhong Yangjie, Liu Jia, Ke Yan, and Liu Meiqi, "Image steganography based on generative implicit neural representation," *arXiv preprint arXiv:2406.01918*, 2024.
- [10] Vincent Sitzmann, Julien Martel, Alexander Bergman, David Lindell, and Gordon Wetzstein, "Implicit neural representations with periodic activation functions," *Advances in neural information processing systems*, vol. 33, pp. 7462–7473, 2020.
- [11] Weina Dong, Jia Liu, Lifeng Chen, Wenquan Sun, Xiaozhong Pan, and Yan Ke, "Implicit neural representation steganography by neuron pruning," 2024.
- [12] Benedetta Tondi, Andrea Costanzo, and Mauro Barni, "Robust dnn watermarking via fixed embedding weights with optimized distribution," *arXiv preprint arXiv:2208.10973*, 2022.
- [13] Monsij Biswal, Tong Shao, Kenneth Rose, Peng Yin, and Sean Mccarthy, "Steganerv: Video steganography using implicit neural representation," in *Proceedings of the IEEE/CVF Conference on Computer Vision and Pattern Recognition*, 2024, pp. 888–898.
- [14] Ben Mildenhall, Pratul P Srinivasan, Matthew Tancik, Jonathan T Barron, Ravi Ramamoorthi, and Ren Ng, "Nerf: Representing scenes as neural radiance fields for view synthesis," *Communications of the ACM*, vol. 65, no. 1, pp. 99–106, 2021.
- [15] Olaf Ronneberger, Philipp Fischer, and Thomas Brox, "U-net: Convolutional networks for biomedical image segmentation," in *Medical image computing and computer-assisted intervention—MICCAI 2015: 18th international conference, Munich, Germany, October 5-9, 2015, proceedings, part III 18*. Springer, 2015, pp. 234–241.
- [16] Chenxin Li, Xinyu Liu, Wuyang Li, Cheng Wang, Hengyu Liu, and Yixuan Yuan, "U-kan makes strong backbone for medical image segmentation and generation," *arXiv preprint arXiv:2406.02918*, 2024.
- [17] Bernhard Kerbl, Georgios Kopanas, Thomas Leimkühler, and George Drettakis, "3d gaussian splatting for real-time radiance field rendering," *ACM Trans. Graph.*, vol. 42, no. 4, pp. 139–1, 2023.
- [18] Yi-Hua Huang, Yang-Tian Sun, Ziyi Yang, Xiaoyang Lyu, Yan-Pei Cao, and Xiaojuan Qi, "Sc-gs: Sparse-controlled gaussian splatting for editable dynamic scenes," in *Proceedings of the IEEE/CVF Conference on Computer Vision and Pattern Recognition*, 2024, pp. 4220–4230.
- [19] Byeonghyeon Lee, Howoong Lee, Xiangyu Sun, Usman Ali, and Eunbyung Park, "Deblurring 3d gaussian splatting," *arXiv preprint arXiv:2401.00834*, 2024.
- [20] Chenxin Li, Brandon Y Feng, Yifan Liu, Hengyu Liu, Cheng Wang, Weihao Yu, and Yixuan Yuan, "Endospase: Real-time sparse view synthesis of endoscopic scenes using gaussian splatting," *arXiv preprint arXiv:2407.01029*, 2024.
- [21] Hengyu Liu, Yifan Liu, Chenxin Li, Wuyang Li, and Yixuan Yuan, "Lgs: A light-weight 4d gaussian splatting for efficient surgical scene reconstruction," *arXiv preprint arXiv:2406.16073*, 2024.
- [22] Zhiwen Fan, Kevin Wang, Kairun Wen, Zehao Zhu, Dejia Xu, and Zhangyang Wang, "Lightgaussian: Unbounded 3d gaussian compression with 15x reduction and 200+ fps," *arXiv preprint arXiv:2311.17245*, 2023.
- [23] Yifan Liu, Chenxin Li, Chen Yang, and Yixuan Yuan, "Endogaussian: Gaussian splatting for deformable surgical scene reconstruction," *arXiv preprint arXiv:2401.12561*, 2024.
- [24] Geoffrey Hinton, "Distilling the knowledge in a neural network," *arXiv preprint arXiv:1503.02531*, 2015.
- [25] Chenxin Li, Mingbao Lin, Zhiyuan Ding, Nie Lin, Yihong Zhuang, Yue Huang, Xinghao Ding, and Liujuan Cao, "Knowledge condensation distillation," in *European Conference on Computer Vision*. Springer, 2022, pp. 19–35.
- [26] Wang Yifan, Felice Serena, Shihao Wu, Cengiz Öztireli, and Olga Sorkine-Hornung, "Differentiable surface splatting for point-based geometry processing," *ACM Transactions on Graphics (TOG)*, vol. 38, no. 6, pp. 1–14, 2019.
- [27] Panwang Pan, Zhiwen Fan, Brandon Y Feng, Peihao Wang, Chenxin Li, and Zhangyang Wang, "Learning to estimate 6dof pose from limited data: A few-shot, generalizable approach using rgb images," in *2024 International Conference on 3D Vision (3DV)*. IEEE, 2024, pp. 1059–1071.
- [28] Chin-Chen Chang, Ju-Yuan Hsiao, and Chi-Shiang Chan, "Finding optimal least-significant-bit substitution in image hiding by dynamic programming strategy," *Pattern Recognition*, vol. 36, no. 7, pp. 1583–1595, 2003.
- [29] Shumeet Baluja, "Hiding images in plain sight: Deep steganography," *Advances in neural information processing systems*, vol. 30, 2017.
- [30] Chenxin Li, Hengyu Liu, Zhiwen Fan, Wuyang Li, Yifan Liu, Panwang Pan, and Yixuan Yuan, "Gaussianstego: A generalizable steganography pipeline for generative 3d gaussians splatting," *arXiv preprint arXiv:2407.01301*, 2024.